Implementation of New Adaptive Cohesive Elements for the Simulation of Delamination in Composite Materials in LS-DYNA

Ahmed Elmarakbi, Ning Hu, Hisao Fukunaga

Departement of Aerospace Engineering, Tohoku University, Sendai, Japan

Summary:

A new 8-node adaptive cohesive element is developed and implemented in LS-DYNA to stabilize the finite element simulations of delamination propagation in composite laminates under transverse loads. In this model, a pre-softening zone is proposed ahead of the existing softening zone. In this pre-softening zone, the initial stiffness and the interface strength are gradually decreased. The onset displacement and the critical energy release rate of the materials are kept constant. The validity of this new model is proved by an excellent agreement between the numerical findings and the experimental results of DCB specimen in Mode-I. The numerical results show that the proposed model brings stable simulations and overcome the numerical instability.

Keywords:

Delamination, Composite laminates, Adaptive cohesive element, Finite element analysis.

1 Introduction

Delamination is one of the predominant forms of failure in laminated composites when subjected to transverse loads and due to the lack of reinforcement in the thickness direction. Delamination can cause a significant reduction in the compressive load-carrying capacity of a structure.

Cohesive elements are widely used, in both forms of continuous interface elements and point cohesive elements, [1-7] at the interface between solid finite elements to predict and to understand the damage behavior in the interfaces of different layers in composite laminates. A main advantage of the use of cohesion elements is the capability to predict both onset and propagation of delamination without previous knowledge of the crack location and propagation direction. However, generally, numerical instabilities frequently occur when using the cohesive interface model to simulate the interface damages. To stabilize the finite element simulations of delamination propagation in composite laminates under transverse loads and to overcome these numerical instabilities, a new 8-node cohesive element model is proposed in this paper. In this model, a pre-softening zone is proposed ahead of the existing softening zone. In this pre-softening zone, the initial stiffness and the interface strength are gradually decreased. The onset displacement corresponding to the onset damage is not changed in the proposed model. Moreover, the critical energy release rate of the materials is kept constant.

To assist in designing laminated composites, finite element simulation is a powerful tool and can be used in the initial design stage without going through multiple-cycles of prototype testing and iterative design changes. Among the various commercial finite element codes, LS-DYNA [8] excels in large deformation transient dynamic problems and impact simulations due to the explicit time integration algorithms within the code. LS-DYNA has a large library of material options which have been widely used in the automobile and aerospace industries. However, continuous cohesive elements are not available within the code.

In this study, the new cohesive element is formulated and implemented in LS-DYNA as a user defined material (UMAT) designed for solid elements. The formulation of this model is fully three dimensional and can simulate mixed-mode delamination. However, the objective of this study is to develop new adaptive cohesive elements able to capture delamination onset and growth under Mode-I loading condition. The capabilities of the proposed elements are proven by comparing the numerical simulations and the experimental results of DCB in Mode-I.

2 Modeling and implementaion of adaptive cohesive elements

2.1 Constitutive equations

The cohesive element is used to model the interface between sublaminates. The elements consists of a zero-thickness volumetric element in which the interpolation shape functions for the top and bottom faces are compatible with the kinematics of the elements that are being connected to it [9]. Cohesive elements are typically formulated in terms of traction vs. relative displacement relationship. In order to predict the initiation and growth of delamination, an 8-node cohesive element shown in Fig .1 is developed and modified to overcome the numerical instabilities.

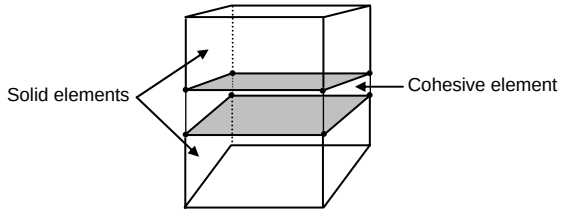

Fig. 1: Eight-node cohesive element.

The need for an appropriate constitutive equation in the formulation of the interface element is fundamental for an accurate simulation of the interlaminar cracking process. A constitutive equation is used to relate the traction to the relative displacement at the interface. The bilinear model is the

simplest model to be used among many strain softening models. Moreover, it has been successfully used by several authors in implicit analyses [10]. However, using the bilinear model leads to numerical instabilities in an explicit implementation. To overcome this numerical instability, a new adaptive model is proposed and presented in this paper.

In this model, a pre-softening zone is proposed ahead of the existing softening zone. In this pre-softening zone, the initial stiffness and the interface strength are gradually decreased. The onset displacement corresponding to the onset damage is not changed in the proposed model. Moreover, the critical energy release rate of the materials is kept constant.

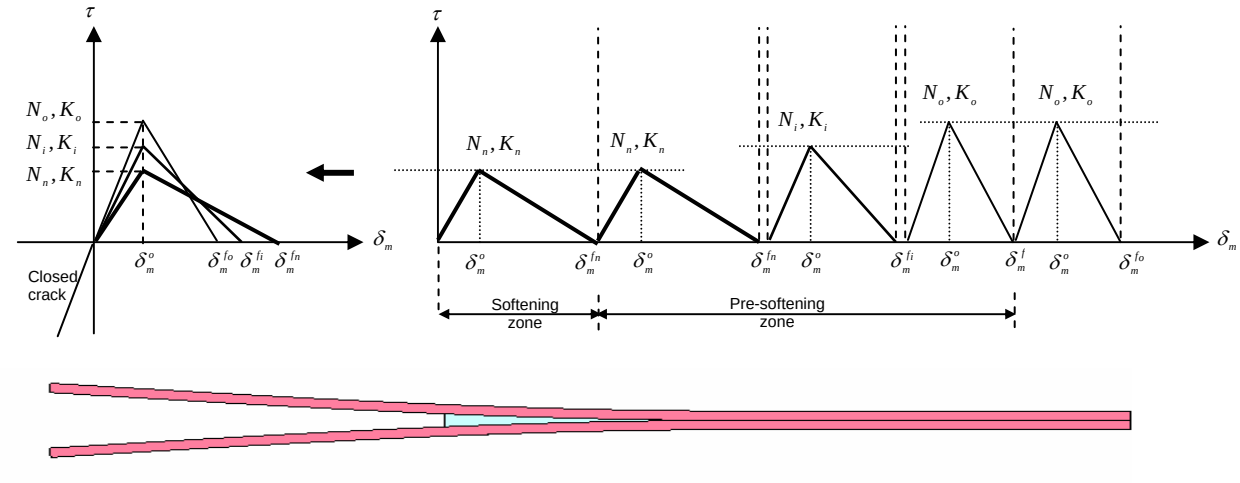

Fig. 2: Adaptive constitutive model for Mode-I.

The adaptive interfacial constitutive response shown in Fig. 2 is implemented as follows:

1. $\delta_m^{\max} < \delta_m^o$, the constitutive equation is given by

$$\tau = K\delta_m \tag{1}$$

where τ is the traction, K is the penalty stiffness and can written as

$$K = \begin{cases} K_o & \delta_m \le 0 \\ K_i & \delta_m^{\max} < \delta_m^o \\ K_n & \delta_m^o \le \delta_m^{\max} < \delta_m^f \end{cases} \tag{2}$$

δ_m is the relative displacement in the interface between the top and bottom surfaces (in this study, it equals the normal relative displacement for Mode-I), δ_m^o is the onset displacement and it is remained constant in the simulation and can be determined as follows:

$$\delta_m^o = \frac{N_o}{K_o} = \frac{N_i}{K_i} = \frac{N_{\min}}{K_{\min}} \tag{3}$$

Were N_o is the initial interface strength, N_i is the updated interface strength in the pre-softening zone, $N_{\min}$ is the minimum limit of the interface strength, K_o is the initial stiffness, K_i is the updated stiffness in the pre-softening zone, and $K_{\min}$ is the minimum value of the stiffness. The $\delta_m^{\max}$ is the max relative displacement of the cohesive element occurs in the deformation history and can be defined as

$$\delta_m^{\max} = \max\left\{\delta_m^{\max}, \delta_m\right\} \tag{4}$$

Using the max value of the relative displacement $\delta_m^{\max}$ rather than the current value δ_m prevents healing of the interface.

The updated stiffness and interface strength are determined in the following forms:

$$N_i = \frac{\delta_m^{\max}}{\delta_m^o}(N_{\min} - N_o) + N_o \ , \ N_o > N_{\min} \tag{5}$$

$$K_i = \frac{\delta_m^{\max}}{\delta_m^o}(K_{\min} - K_o) + K_o \ , \ K_o > K_{\min} \tag{6}$$

The energy release rate for Mode-I G_{IC} is also remained constant. Therefore, the final displacements associated to the complete decohesion $\delta_m^{f_i}$ are adjusted as shown in Fig. 2 as

$$\delta_m^{f_i} = \frac{2G_{IC}}{N_i} \tag{7}$$

Once the displacement of the interface reaches the softening process, the current strength N_n and stiffness K_n which are almost equal to $N_{\min}$ and $K_{\min}$, respectively, will be used in the softening zone.

2. $\delta_m^o \le \delta_m^{\max} < \delta_m^f$, the constitutive equation is given by

$$\tau = (1-d)K\delta_m \tag{8}$$

Where d is the damage variable and can be defined as

$$d = \frac{\delta_m^f(\delta_m^{\max} - \delta_m^o)}{\delta_m^{\max}(\delta_m^f - \delta_m^o)}, \quad d \in [0,1] \tag{9}$$

2.2 Implementation

The proposed cohesive element is implemented in LS-DYNA finite element code as a user defined material (UMAT) using the standard library 8-node solid brick element. This approach for the implementation requires modeling the resin rich layer as a non-zero thickness medium. In fact, this layer has a finite thickness and the volume associated with the cohesive element can in fact set to be very small by using a very small thickness (e.g. 0.01 mm). To verify these procedures, the crack growth along the interface of a double cantilever beam (DCB) is studied. The two arms are modeled using standard LS-DYNA 8-node solid brick elements and the interface elements are developed in FORTRAN subroutine using the algorithm shown in Fig.3.

The LS-DYNA code calculates the strain increments for a time step and passes them to the UMAT subroutine at the beginning of each time step. The material constants, such as the stiffness and strength, are read from the LS-DYNA input file by the subroutine. The current and maximum relative displacements are saved as history variables which can be read in by the subroutine. Using the history variables, material constants, and strain increments, the subroutine is able to calculate the stresses at the end of the time step by using the form of constitutive equations. The subroutine then updates and saves the history variables for use in the next time step, and outputs the calculated stresses. Note that the *DATABASE_EXTENT_BINARY command is requires to specify the storage of history variables in the output file.

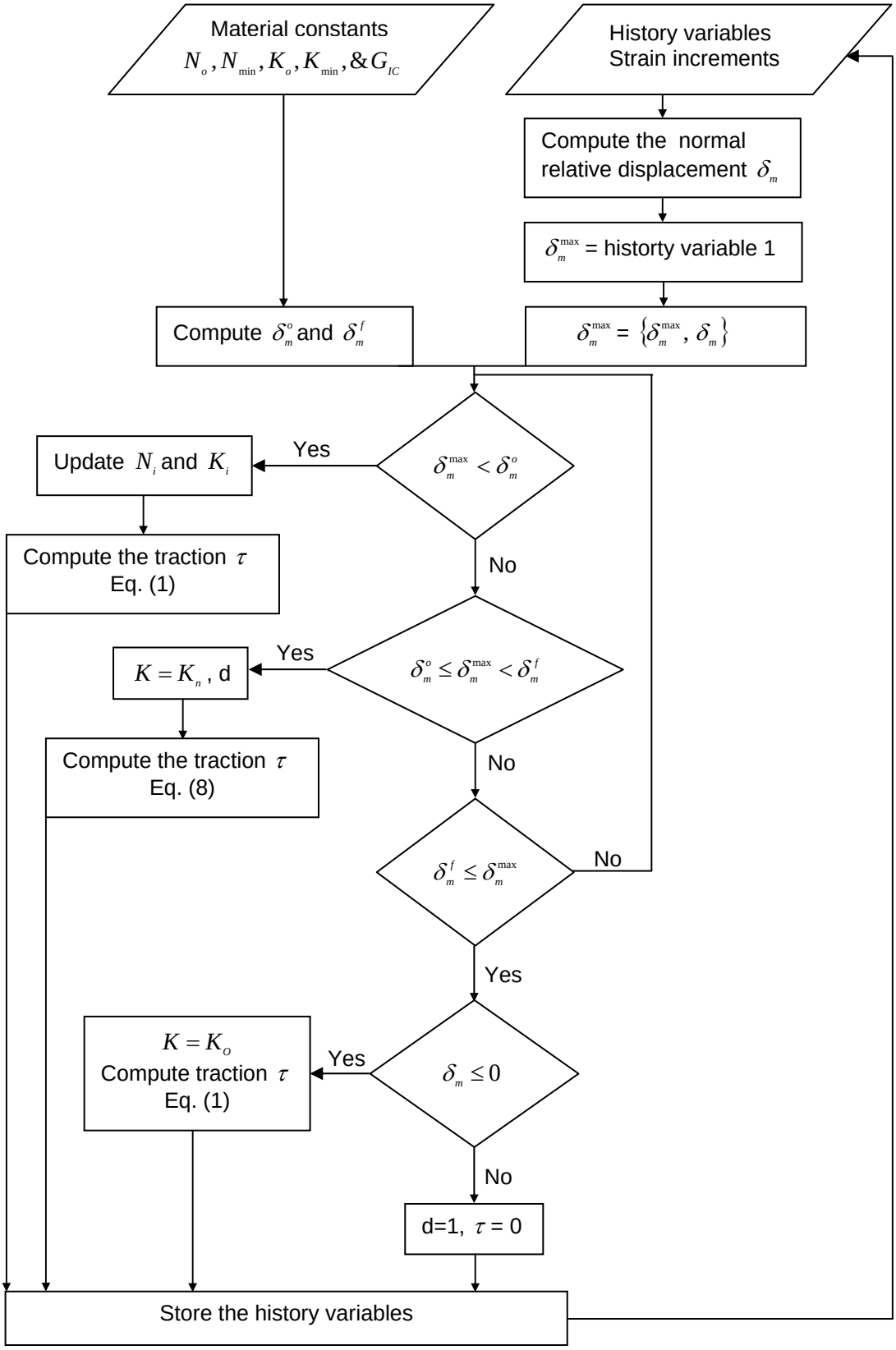

Fig. 3: Flow chart for traction computation in Mode-I.

3 Numerical simulations

The DCB specimen is made of a unidirectional fiber-reinforced laminate containing a thin insert at the mid-plan near the loaded end. A 15 cm long specimen, 2 cm wide and composed of two 1.98 mm thick plies of unidirectional material shown in Fig. 4 was tested by Morais [11]. The initial crack length is 5.5 cm. A displacement rate of 10 mm/sec is applied to the appropriate points of the model. The properties of both carbon fiber-reinforced epoxy material and the interface are given in Table 1.

Table 1. Properties of both Carbon fiber-reinforced epoxy material and Specimen interface

Carbon fiber- reinforced epoxy material	DCB specimen interface
ρ =1444 kg/m^3	G_{IC} = 0.378 kJ/m^2
E_{11} = 150 MPa, E_{22} = E_{33} = 11 MPa	K_o = 3x10^4 N/mm^3
υ_{12} = υ_{13} = 0.25 , υ_{23} = 0.45	N_o = 45 MPa Case I
G_{12} = G_{13} = 6.0 MPa, G_{23} = 3.7 MPa	N_o = 60 MPa Case II

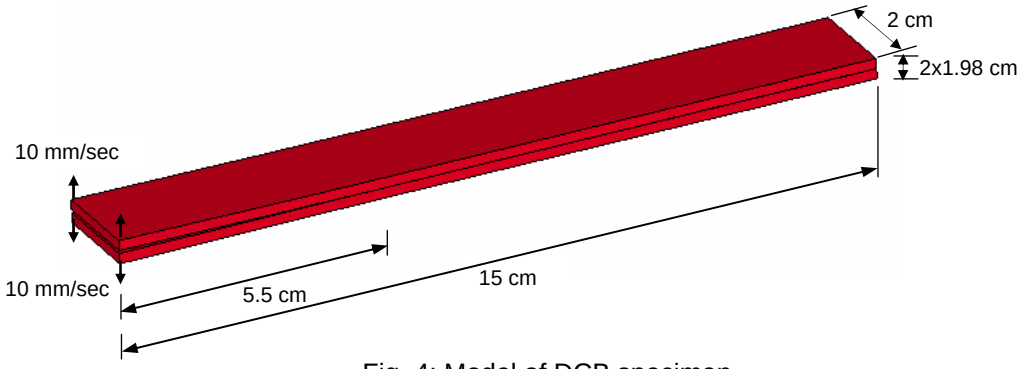

Fig. 4: Model of DCB specimen.

The LS-DYNA finite element model, which is shown deformed in Fig. 5, consists of two layers of fully integrated S/R 8-noded solid elements. Each arm of the specimen is modeled using fully integrated S/R 8-noded solid elements, with 3 elements across the thickness. Two cases of mesh modeling are used in the initial analysis, namely: Case A, which includes eight elements across the width, and Case B, which includes one element across the width, respectively. The two cases are compared using the adaptive model with mesh size of 1 mm to figure out the anticlastic effects.

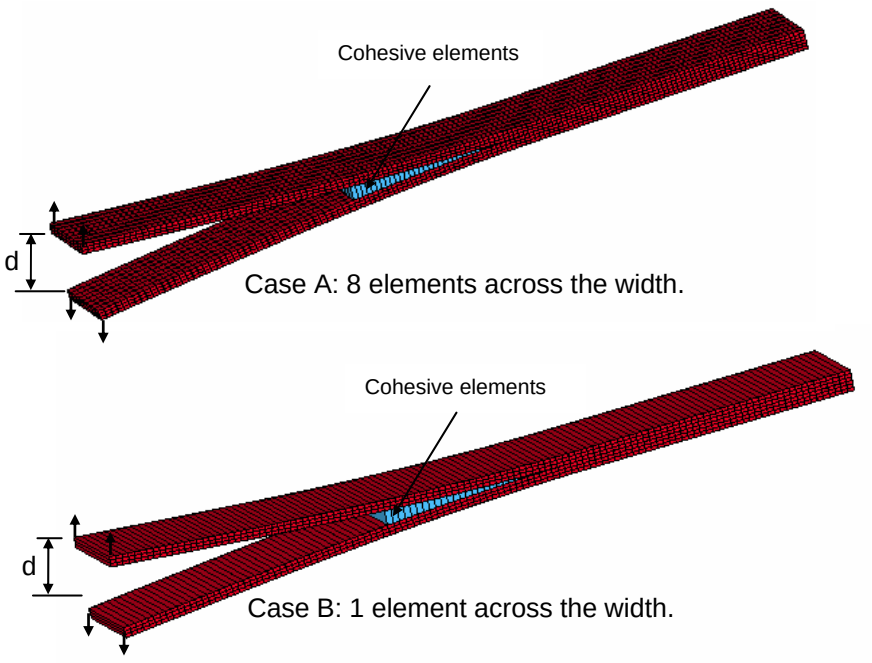

Fig. 5: LS-DYNA finite element model of the deformed DCB specimen.

A plot of a reaction force as a function of the applied end displacement is shown in Fig. 6. It is clearly shown that both cases bring similar results with peak load value of 64 N. Therefore, the anticlastic effects are neglected and only one element (Case B) is used across the width in the following analyses.

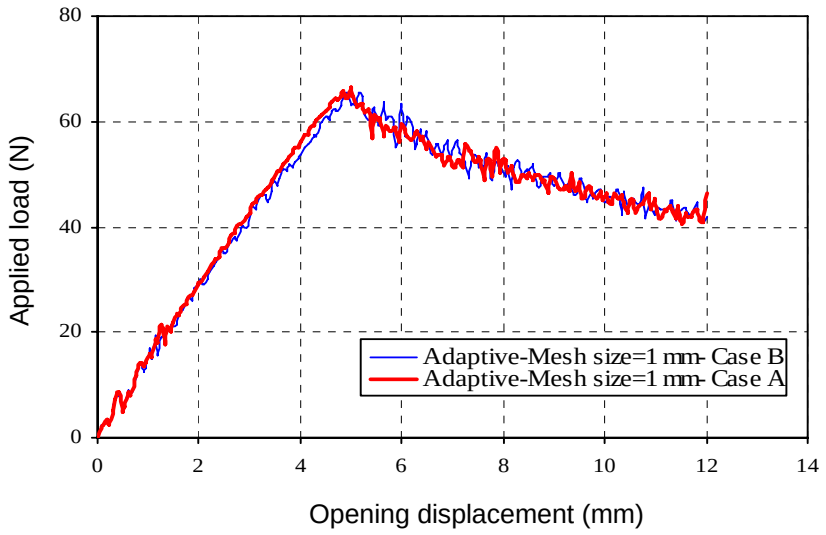

Fig. 6: Load-displacement curves for a DCB specimen in both cases A and B.

The influence of the new adaptive cohesive element is determined in the following analyses using different mesh sizes in both values of the normal interface strengths (Case I, N_0 = 45 MPa; Case II, N_0 = 60 MPa). Different cases are considered in this study and given in Table 2.

Table 2. Different cases of analyses

Case 1	Mesh size = 2 mm	N_o = 45 MPa, N_{min} = 15 MPa	K_o = 3x10^4 N/mm^3, K_{min} = 1x10^4 N/mm^3
Case 2	Mesh size =1.25 mm		
Case 3	Mesh size = 1 mm		
Case 4	Mesh size = 0.75 mm		
Case 5	Mesh size = 0.5 mm		
Case 6	Mesh size = 1 mm	N_o = 45 MPa, N_{min} = 22.5 MPa	K_o = 3x10^4 N/mm^3, K_{min} =1.5x10^4 N/mm^3
Case 7	Mesh size = 1 mm	N_o = 45 MPa, N_{min} = 10 MPa	K_o = 3x10^4 N/mm^3, K_{min} = 0.667x10^4 N/mm^3
Case 8	Mesh size = 1 mm	N_o = 60 MPa, N_{min} = 30 MPa	K_o = 3x10^4 N/mm^3, K_{min} = 1.5x10^4 N/mm^3

The aim of the first five cases is to study the effect of the element size with constant values of interface strength and stiffness on the load-displacement relationship. Different element sizes are used along the interface spanning from very small size of 0.5 mm to coarse mesh of 2 mm. Moreover, Cases 3, 6, and 7 are to study the effect of the value of minimum interface strength on the results, Finally, cases 6 and 8 are to find out the effect of the high interfacial strength.

Figs.7-11 show the load-displacement curves for both normal (bilinear) and adaptive cohesive elements in the first five cases with different element sizes. Fig. 7 clearly shows that the bilinear formulation results in a severe instability once the crack starts propagating. However, the adaptive constitutive law is able to model the smooth, progressive crack propagation. It is worth mentioning that the bilinear formulation brings smooth results by decreasing the element size. And it is clearly noticeable from Fig. 11 that both bilinear and adaptive formulations are found to be stable in Case 5 with very small element size. This indicates that the higher accuracy using bilinear formulation requires the smallest element size in the softening zone. However, this leads to large computational costs compare to case 1. On the other hand, Fig. 12, which presents the load-displacement curves, obtained with the use of the adaptive formulation in the first five cases, show a great agreement of the

results regardless the mesh size. Therefore, the new adaptive model can be used with considerably large mesh size and the computational cost will be greatly minimized.

The load-displacement curves obtained from the numerical simulation of Cases 3, 6 and 7 are presented in Fig. 13 together with experimental data [12]. It can be seen that an excellent agreement between the experimental data and the numerical predictions is obtained. The average maximum load obtained in the experiments is 62.5 N, whereas the average maximum load predicted form the three cases is 65 N. It can be observed that numerical curves slightly overestimate the load. It is worth noting that there is a very slight difference in the numerical analysis in the three cases, however, the curve becomes a bit smoother once the minimum interface strength lowered.

Fig. 14 show the load-displacement curves of the numerical simulations obtained using the bilinear formulation in both cases case 6 and 8. The bilinear formulations results in a severe instabilities once the crack starts propagation. It is also shown that a higher maximum traction (case 8) resulted in a more severe instability compared to a lower maximum traction (case 6). However, as shown in Fig. 15, the load-displacement curves of the numerical simulations obtained using the adaptive formulations are very similar in both cases. The maximum load obtain from case 8 is found to be 69 N while in case 6, the maximum load obtained is 66 N. The adaptive formulation are able to model the smooth, progressive crack propagation and also to give accurate results compared to the experimental results.

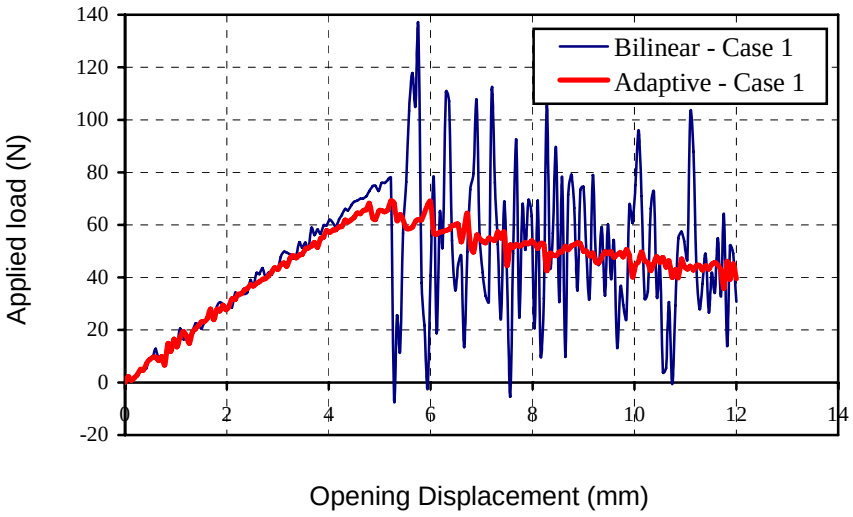

Fig. 7: Load-displacement curves obtained using both Bilinear and Adaptive formulations-Case 1.

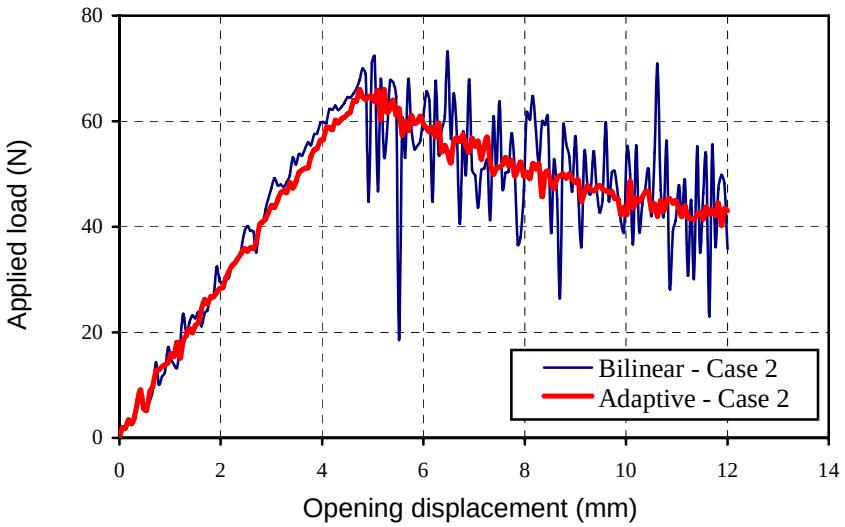

Fig. 8: Load-displacement curves obtained using both Bilinear and Adaptive formulations-Case 2.

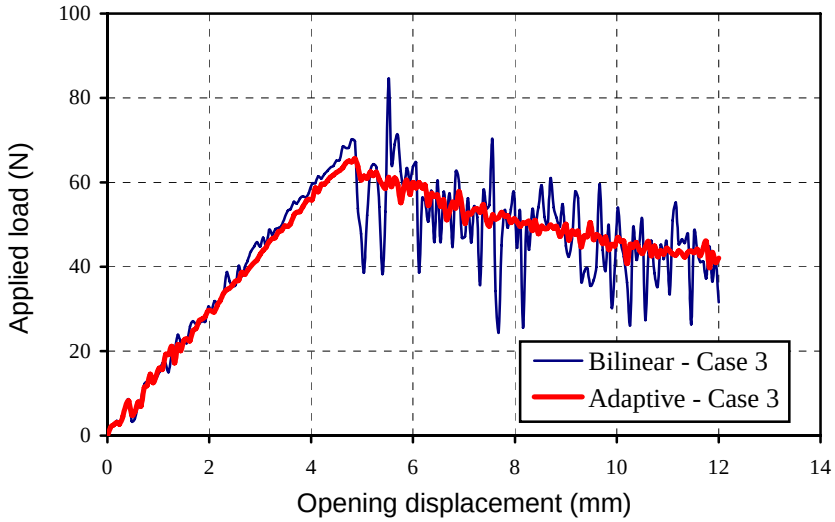

Fig. 9: Load-displacement curves obtained using both Bilinear and Adaptive formulations-Case 3.

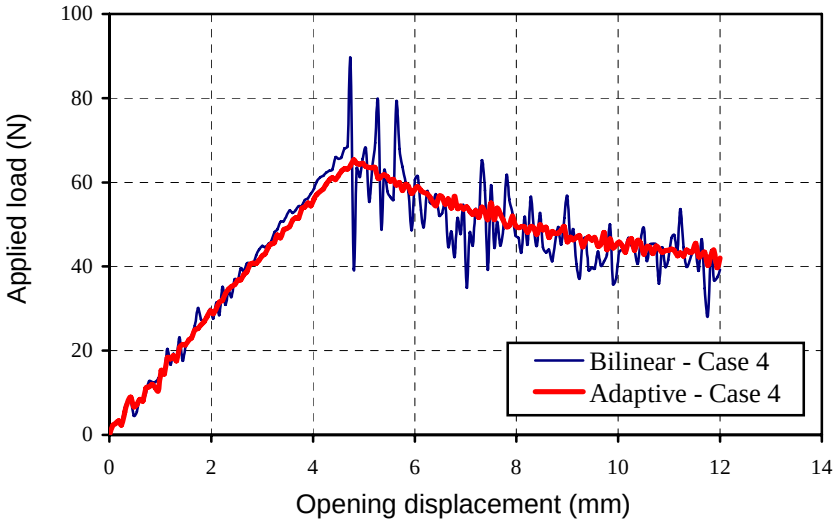

Fig. 10: Load-displacement curves obtained using both Bilinear and Adaptive formulations-Case 4.

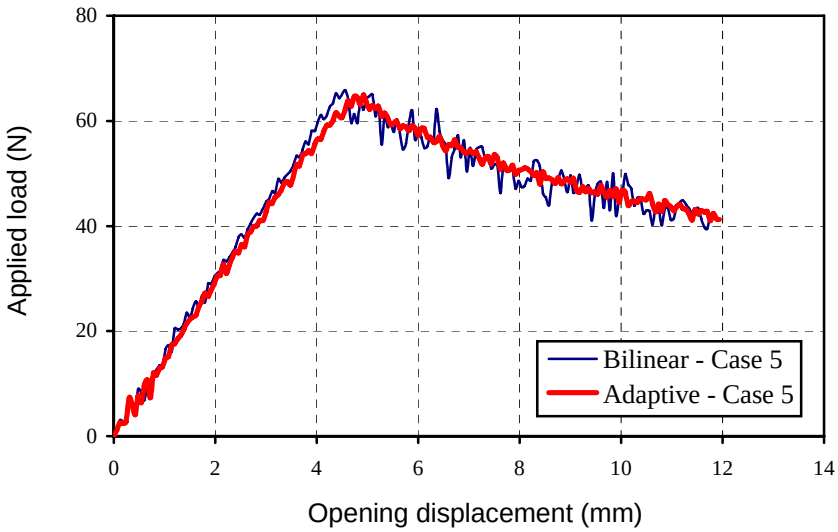

Fig. 11: Load-displacement curves obtained using both Bilinear and Adaptive formulations-Case 5.

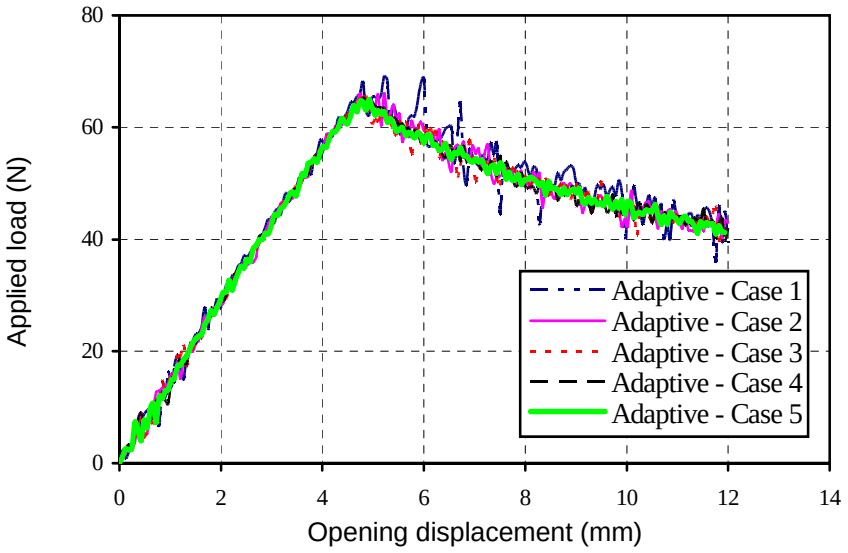

Fig. 12: Load-displacement curves obtained using the Adaptive formulation-Cases 1-5.

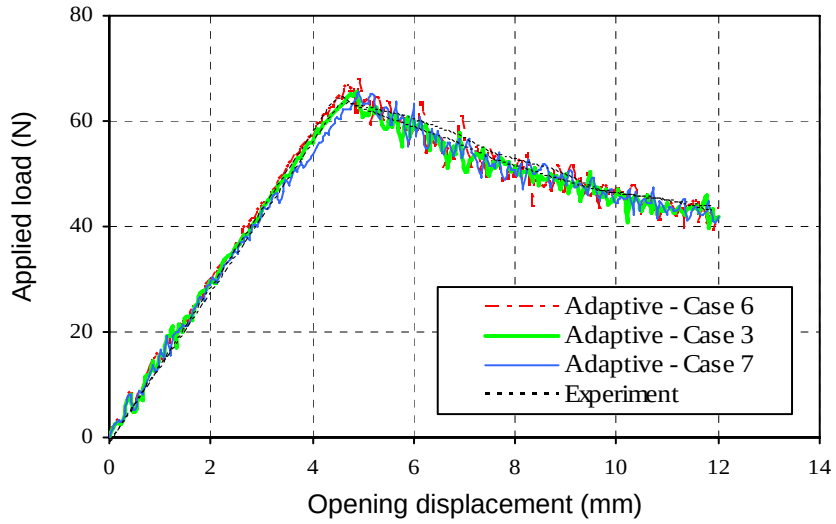

Fig. 13: Comparison of the experimental and numerical Load-displacement curves obtained using the Adaptive formulation-Cases 3, 6 and 7.

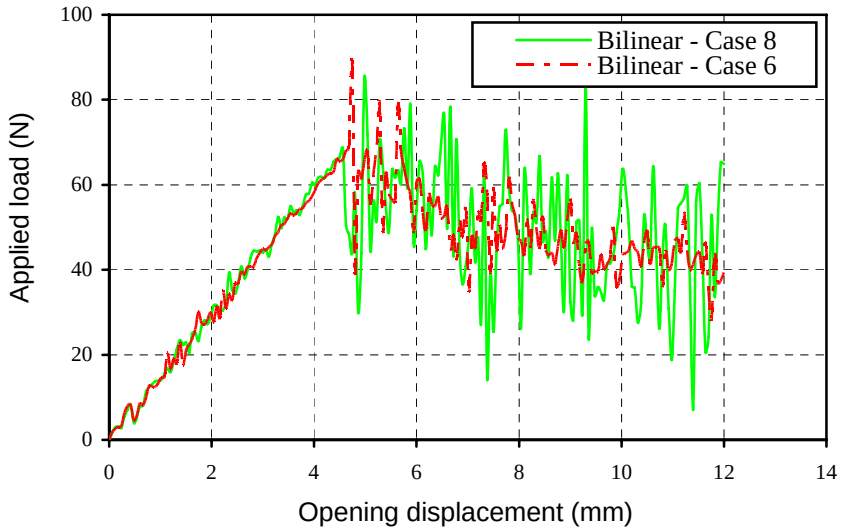

Fig. 14: Load-displacement curves obtained using the Bilinear formulation- Cases 6 and 8.

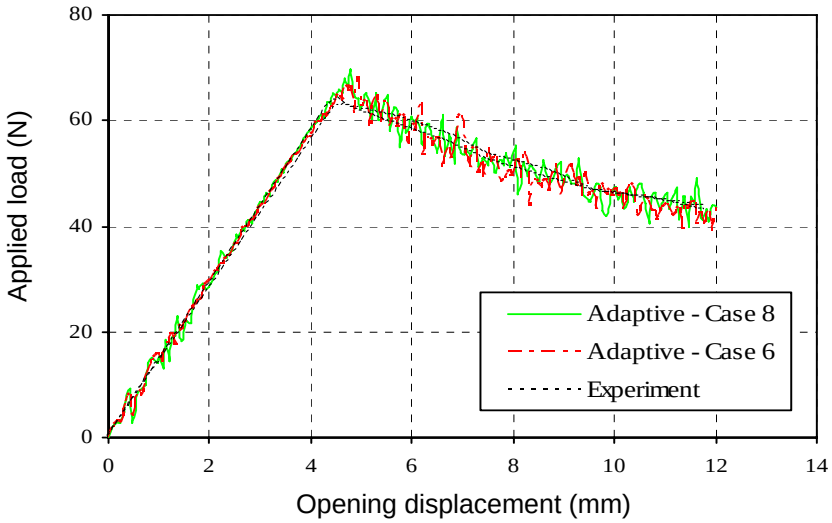

Fig. 15: Comparison of the experimental and numerical Load-displacement curves obtained using the Adaptive formulation-Cases 6 and 8.

4 Conclusions

A method for simulation of progressive delamination based on cohesive elements is presented. A new adaptive cohesive element is developed and implemented in LS-DYNA to overcome the numerical insatiability occurred using the bilinear cohesive model. The formulation is fully three dimensional, and can be simulating mixed-mode delmaination, however, in this study, only DCB test in Mode-I is used as a reference to validate the numerical simulations. The numerical simulation shows that the new model is able to model the smooth, progressive crack propagation. Furthermore, the new model can be effectively used in a range of different element size (reasonably coarse mesh) and can save a large amount of computation. The capability of the new mode is proved by the great agreement obtained between the numerical simulations and the experimental results.

5 Acknowledgement

The authors wish to acknowledge the financial support provided for this ongoing research by Japan Society for the Promotion of Science (JSPS).

6 References

[1] Camanho, P, Davila, C, and Ambur, D: “Numerical simulation of delamination growth in composite materials”, NASA-TP-211041, 2001, 1-19.

[2] de Moura, M, Goncalves, J, Marques, A, and de Castro, P: “Modeling compression failure after low velocity impact on laminated composites using interface elements”, Journal of Composites Materials, 31, 1997, 1462-1479.

[3] Reddy Jr, E, Mello, F, and Guess, T: “Modeling the initiation and growth of delaminations in composite structures”, Journal of Composite Materials, 31, 1997, 812-831.

[4] Chen, J, Crisfield, M. Kinloch, A, Busso, E, Matthews, F, and Qiu, Y: “Predicting progressive delamination of composite material specimens via interface elements”, Mechanics of Composite Materials and Structures, 6, 1999, 301-317.

[5] Petrossian, Z, and Wisnom, M: “Prediction of delamination initiation and growth from discontinues plies using interface elements”, Composites-Part A, 29, 1998, 503-515.

[6] Cui, W, and Wisnom, M: “A combined stress-based and fracture mechanics-based model for predicting delamination in composites”, Composites, 24, 1993, 467-474.

[7] Shahwan, K, and Wass, A: “Non-self-similar decohesion along a finite interface of unilaterally constrained delaminations”, Proceeding of the Royal Society of London, 453, 1997, 515-550.

[8] Livermore Software Technology Corporation, California, USA, LS-DYNA 970; 2005.

[9] Davila, C, Camanho, P, de Moura, M: “ Mixed-mode decohesion elements for analyses of progressive delamination”, 42nd AIAA/ASME/ASCE/AHS/ASC Structures, Structural Dynamics and Material Conference, Washington, USA, AIAA-01-1486, 2001,1-12.

[10] Pinho, S, Lannucci, P, and Robinson, P: “Formulation and implementation of decohesion elements in an explicit finite element code”, Composites-Part A, 37, 2006, 778-789.
[11] Morais, A, Marques, A, and de Castro, P: “Estudo da aplicacao de ensaios de fractura interlaminar de mode I a laminados compositos multidireccionais”, Proceedings of the 7as jornadas de fractura, Sociedade Portuguesa de Materiais, Portugal, 2000, 90-95.
[12] Camanho, P, and Davila, C: “Mixed-mode decohesion finite elements for the simulation of delamination in composite materials”, NASA/TM-2002-211737, 2002, 1-37.

